

Capped-Tetrahedrally Coordinated Fe(II) and Co(II) Complexes Using a “Click”-Derived Tripodal Ligand: Geometric and Electronic Structures

David Schweinfurth,[†] Serhiy Demeshko,^{||} Marat M. Khusniyarov,[§] Sebastian Dechert,^{||} Venkatanarayana Gurram,[⊥] Michael R. Buchmeiser,[⊥] Franc Meyer,^{||} and Biprajit Sarkar^{*,†,‡}

[†]Institut für Anorganische Chemie, Universität Stuttgart, Pfaffenwaldring 55, D-70550, Stuttgart, Germany

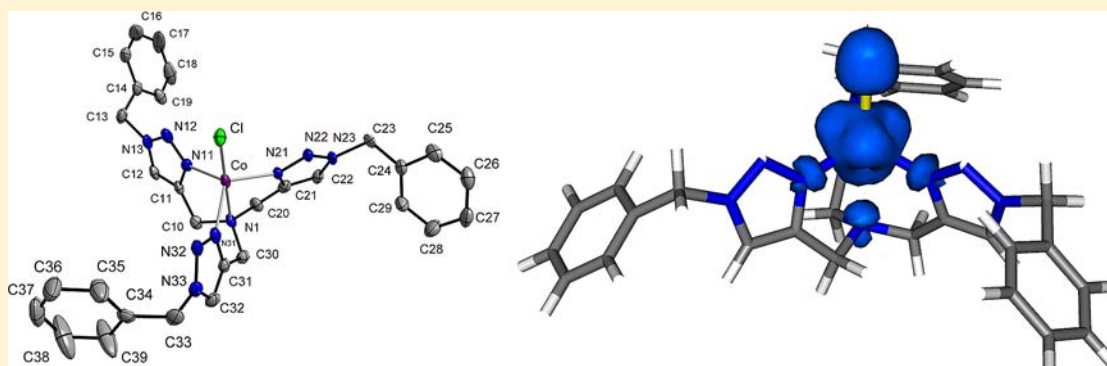
[‡]Institut für Chemie und Biochemie, Anorganische Chemie, Freie Universität Berlin, Fabeckstrasse 34-36, D-14195, Berlin, Germany

[§]Department Chemie und Pharmazie, Friedrich-Alexander Universität Erlangen-Nürnberg, Egerlandstrasse 1, D-91058, Erlangen, Germany

^{||}Institut für Anorganische Chemie, Georg-August Universität Göttingen, Tammanstrasse 4, D-37077, Göttingen, Germany

[⊥]Institut für Polymerchemie, Universität Stuttgart, Pfaffenwaldring 55, D-70550, Stuttgart, Germany

Supporting Information



ABSTRACT: The ‘Click’-derived tripodal ligand tris[(1-benzyl-1*H*-1,2,3-triazole-4-yl)methyl]amine, tbta, was used to synthesize the complexes [Fe(tbta)Cl]BF₄, **1**, and [Co(tbta)Cl]BF₄, **2**. Both complexes were characterized by ¹H NMR spectroscopy and elemental analysis. Single-crystal X-ray structural determination of **2** shows a 4 + 1 coordination around the cobalt(II) center with a rather long bond between Co(II) and the central amine nitrogen atom of tbta. Such a coordination geometry is best described as capped tetrahedral. **1** and **2** are thus the first examples of pseudotetrahedrally coordinated Fe(II) and Co(II) complexes with tbta. A combination of SQUID susceptibility, EPR spectroscopy, Mössbauer spectroscopy, and DFT calculations was used to elucidate the electronic structures of these complexes and determine the spin state of the metal center. Comparisons are made between the complexes presented here with related complexes of other ligands such as tris(2-pyridylmethyl)amine, tmpa, hydrotris(pyrazolyl) borate, Tp, and tris(2-(1-pyrazolyl)methyl)amine, amtp. **1** and **2** were tested as precatalysts for the homopolymerization of ethylene, and both complexes delivered distinctly different products in this reaction. Blind catalyst runs were carried out with the metal salts to prove the importance of the tripodal ligand for product formation.

INTRODUCTION

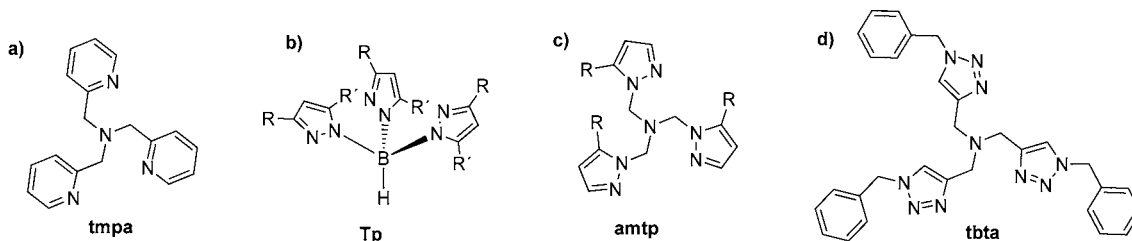
The Cu(I)-catalyzed cycloaddition reaction between azides and alkynes has been widely used by synthetic chemists in recent years.^{1–3} The resulting 1,2,3-triazole-containing compounds are becoming increasingly popular ligands in coordination chemistry.⁴ The bidentate and tridentate forms of such ligands have been compared to the extensively used 2,2'-bipyridine and 2,2',6',2''-terpyridine ligands.^{5–17} The potentially tetradentate ligand tris[(1-benzyl-1*H*-1,2,3-triazole-4-yl)methyl]amine, tbta,^{18,19} is analogous to tris(2-pyridylmethyl)amine, tmpa, hydrotris(pyrazolyl) borate, Tp, and tris(2-(1-pyrazolyl)methyl)amine, amtp (Scheme 1).

Metal complexes of tmpa have been used in the context of bioinorganic research as well as for studying electron transfer.^{20–24} The ligand Tp has been used for a variety of purposes by coordination and bioinorganic chemists, including activation of small molecules by its metal complexes.^{25–28} Various metal complexes of the ligand amtp have been reported in the literature.^{29–33} The modular synthetic route offered by the “Click” method helps in easy modification of the steric and electronic properties of such ligands and makes a library of

Received: February 21, 2012

Published: June 25, 2012

Scheme 1. Analogy between tbta and Related Ligands



ligands easily accessible.^{18,19} We made use of this protocol and recently reported on 6-fold-coordinated Co(II) complexes with tbta that showed coordination ambivalence and spin crossover.³⁴ There have also been reports on Cu(I) complexes of tbta.^{35,36}

In the following we present the synthesis of the first examples of pseudotetrahedral-coordinated iron and cobalt complexes [Fe(tbta)Cl]BF₄, **1**, and [Co(tbta)Cl]BF₄, **2**, with the tripodal ligand tbta. Characterization of compounds **1** and **2** by ¹H NMR spectroscopy, elemental analyses, X-ray crystallography, SQUID susceptometry, EPR spectroscopy, Mössbauer spectroscopy, and DFT calculations will be presented. These results will be used to elucidate the geometric and electronic structures of the complexes. Results on the use of **1** and **2** as precatalysts for homopolymerization of ethylene will also be presented.

RESULTS AND DISCUSSION

Synthesis and Characterization of Complexes and Crystal Structures of tbta and 2. The ligand tbta was synthesized by following methods reported in the literature.³⁷ We were able to crystallize tbta for single-crystal diffraction studies. tbta crystallizes in the *P2₁/n* space group (Figure S1, Supporting Information). The bond lengths inside the 1,2,3-triazole rings are very similar to those observed for other ligands containing such a ring.^{15,16}

Access to **1** and **2** was achieved using a mixture of dichloride and tetrafluoroborate salts of the respective metals and tbta in CH₃CN (see Experimental Section). Synthesis of **1** required the use of an inert atmosphere possibly because of the sensitivity of the Fe(II) centers in the salts and such compounds toward oxidation and hydration. In contrast, complex **2** could be synthesized under air.

Crystals of **2** suitable for single-crystal diffraction studies were obtained by slow diffusion of diethyl ether into an acetonitrile solution at ambient temperatures. Complex **2** crystallizes in the orthorhombic *Pnn2* space group. The cobalt center in **2** is coordinated by one nitrogen atom from each of the three triazole rings of tbta (Figure 1 and Table 1); the distances are as follows: Co–N11, 2.037(3) Å; Co–N21, 2.026(3) Å; Co–N31, 2.035(3) Å. Additionally, there is a chloride ligand with a Co–Cl distance of 2.264(1) Å. Finally, there is a relatively long bond between the cobalt center and the central amine nitrogen of tbta with a Co–N1 distance of 2.350(3) Å. The angles between the triazole nitrogen atoms and cobalt are in the range of 113–114°, those between the triazole nitrogen atoms, cobalt, and chloride are in the range 104–106° (Table S3, Supporting Information). The cobalt center is 0.525(1) Å above the plane containing the three triazole nitrogen-donor atoms. All of the above data point to a 4 + 1 coordination at the cobalt center, and hence, the coordination geometry around the cobalt center is best described as capped tetrahedral.

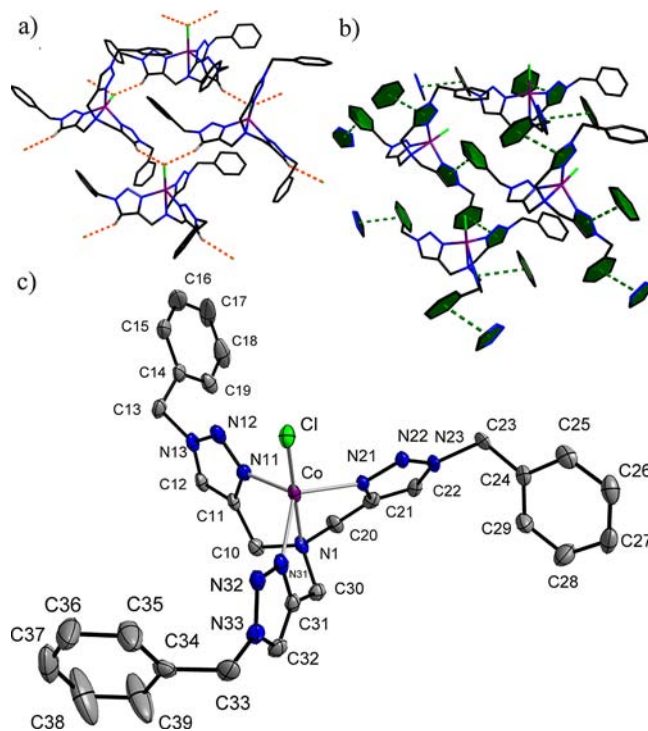


Figure 1. (a) C–H···Cl interactions in **2** in the solid state. (b) π – π interaction in **2** in the solid state. (c) ORTEP plot of **2** drawn at 50% ellipsoid probability; hydrogen atoms and counterions are omitted for clarity.

Table 1. Selected Bond Lengths of **2** (in Angstroms)^a

| | |
|---------------------|-----------|
| Co–Cl | 2.2638(8) |
| Co–N1 | 2.350(3) |
| Co–N11 | 2.037(3) |
| Co–N21 | 2.026(3) |
| Co–N31 | 2.035(3) |
| Cl···H12A | 2.7194(9) |
| Cl···H22A | 2.7322(9) |
| Triazole1···Phenyl2 | 3.679 |
| Triazole3···Phenyl1 | 3.698 |

^aTriazole2 is involved in binding the BF₄[–] anion.

For comparison, the literature reported Co(II) complex [Co(tmpa)Cl]⁺ with tmpa is better described with a coordination geometry of trigonal bipyramidal.^{38–40} The Co–N distances to the pyridine rings of tmpa in that complex are slightly longer than the Co–N(triazole) distances observed in the case of **2**. The main difference, however, is the Co–N(amine) distance, which in the present case is 2.350(3) Å. For [Co(tmpa)Cl]⁺ the corresponding distance is 2.184(6) Å.⁴⁰ Thus, the central amine nitrogen binds much more strongly to

the Co(II) center in $[\text{Co}(\text{tmpa})\text{Cl}]^+$ as compared to **2**. Another ligand that is similar to *tbta* and *tmpa* is *amtp* (Scheme 1), and five-coordinated complexes of the form $[\text{Co}(\text{amtp})\text{Cl}]^+$ have also been reported with that ligand.^{29–33} In one such complex with $R = \text{H}$ in *amtp* the Co(II) center is coordinated in a pseudotetrahedral fashion as in the case of **2**.⁴¹ The distances between Co(II) and the pyrazol N donors are slightly shorter than the corresponding Co–N(triazole) distances in **2**. The Co–N(amine) distance in the case of $[\text{Co}(\text{amtp})\text{Cl}]^+$ is 2.393(4) Å and hence comparable to **2**. Thus, in **2** and $[\text{Co}(\text{amtp})\text{Cl}]^+$ the coordination around the metal center is comparable. However, for $[\text{Co}(\text{tmpa})\text{Cl}]^+$ the ligand *tmpa* is coordinated to the Co(II) center in a more compact manner. The ligand *Tp* (Scheme 1) in complex $[\text{Co}(\text{Tp})\text{Cl}]$ displays Co–N(pyrazol) distances that are comparable to $[\text{Co}(\text{amtp})\text{Cl}]^+$ and the corresponding Co–N(triazole) distances in **2**.^{25,26,42,43} The coordination around the Co(II) center in $[\text{Co}(\text{Tp})\text{Cl}]$ has thus also been described as pseudotetrahedral in the literature.⁴³ A pseudotetrahedral coordination similar to that in **2** has also recently been observed for a 5-fold-coordinated Co(II) complex with a tris(1,2,3-triazole) motif built on an azatriquinacene platform.⁴⁴

The presence of three nitrogen atoms within a five-membered ring makes the C–H group of 1,2,3-triazoles highly acidic.⁴⁵ In the case of **2**, the C–H groups of triazoles and the chlorides bound to cobalt are involved in extended hydrogen bonding in the solid state as shown in Figure 1a. Relevant distances are Cl–H12A = 2.719(1) Å and Cl–H22A = 2.732(1) Å. There are further π – π stackings between the triazole rings and phenyl rings of an adjacent molecule (Figure 1b and Table S2, Supporting Information). Additionally, one triazole ring from each molecule is also involved in a C–H...F interaction with the BF_4^- counterions.

Despite several attempts, we were not able to obtain suitable single crystals for X-ray structure determination of **1**. Hence, to obtain an idea about the local symmetry around the metal centers, ¹H NMR spectroscopy was performed on both **1** and **2**. ¹H NMR data is consistent with the highly paramagnetic nature of the Fe(II) and Co(II) centers in **1** and **2** with the proton signals displaying large paramagnetic shifts and broadening (Experimental Section). This broadening results in the loss of the multiplicities that would otherwise be expected for certain signals of the *tbta* ligand. The ¹H NMR spectra of both **1** and **2** shows six proton resonances, suggesting that the complexes possess a 3-fold symmetry with respect to the *tbta* ligand (three signals from the phenyl rings and one each from the benzyl–methylene, triazole C–H, and the methylene groups attached to the central amine atom). Exchange between the triazole(benzyl) arms averages their environments in solution on the NMR time scale. Such a phenomenon has recently been reported for similar Co(II) complexes of the *tmpa* ligand.⁴⁶ The paramagnetic shifts of the signals seem to correlate with their distances from the paramagnetic metal centers. Thus, the resonances for the aromatic protons of the benzyl ring as well as the methylene protons of the benzyl groups are largely in the expected region (Experimental Section). However, the signals corresponding to the C–H group of the triazole rings and the methylene groups attached to the central amine nitrogen atoms are highly paramagnetically shifted. The appearance of the same number of signals in the ¹H NMR spectrum of **1** and **2** shows the 3-fold symmetry of the *tbta* ligand in both complexes and gives confidence that the coordination around the Fe(II) center in **1**

is similar to that of the Co(II) center in **2** for which we have structural evidence from single-crystal X-ray diffraction studies.

Magnetic and Spectroscopic Investigation and DFT Calculations. SQUID susceptometric measurements were carried out on **1** and **2** in order to investigate their magnetic properties. **1** and **2** show magnetic moments at 300 K that correspond to $S = 2$ and $3/2$ ground states, respectively (Figure 2). Similar values have been reported in the literature for the

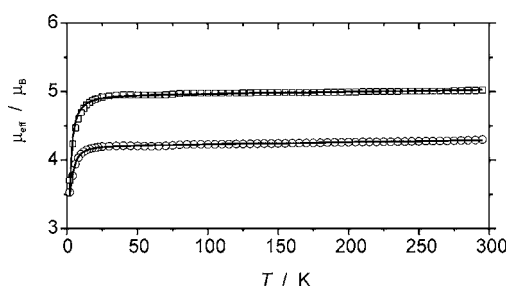


Figure 2. Plot of μ_{eff} vs T for **1** (top) and **2** (bottom) at 0.5 T; solid lines represent calculated curve fits.

corresponding five-coordinate Fe(II) and Co(II) complexes with *tmpa* and *amtp*.^{29–33,40} Magnetic moments for both compounds remain constant on cooling until about 20 K. Below 20 K a slight dip in the magnetic moment is observed that is likely due to zero-field splitting. Magnetic parameters were determined using a fitting procedure to the appropriate spin Hamiltonian for zero-field splitting and Zeeman interaction and including a term for temperature-independent paramagnetism (*TIP*). The best simulation parameters are $g = 2.02$, $|D| = 5.0 \text{ cm}^{-1}$, and $TIP = 3.7 \times 10^{-4} \text{ cm}^3 \text{ mol}^{-1}$ for **1** and $g = 2.17$, $|D| = 4.6 \text{ cm}^{-1}$, and $TIP = 3.2 \times 10^{-4} \text{ cm}^3 \text{ mol}^{-1}$ for **2**. Magnetic data thus suggest the presence of high-spin (HS) Fe(II) and Co(II) centers in **1** and **2**, respectively.

Mössbauer spectroscopy is known to be an extremely useful tool for determination of the oxidation and spin states of iron centers, and EPR spectroscopy is known to be helpful for investigating the spin states of cobalt centers. Thus, in order to further probe the oxidation and spin states of **1** and **2**, Mössbauer and EPR spectroscopies were, respectively, used. The ⁵⁷Fe Mössbauer spectrum of **1** (Figure 3) shows a single quadrupole doublet with an isomer shift $\delta = 1.02 \text{ mm}\cdot\text{s}^{-1}$ and a quadrupole splitting $\Delta E_Q = 3.14 \text{ mm}\cdot\text{s}^{-1}$, which corroborates that the iron ion is in the HS d^6 configuration. The X-band EPR spectrum of **2**, recorded at 110 K, shows a broad signal with a virtually axial g splitting. The spectrum could be simulated using g values of 4.33, 4.20, and 2.17 (Figure 3). The spectrum and g values are typical for a HS Co(II) center, where in the X band usually transitions corresponding to the $m_S = \pm 1/2$ manifold are observed.

In order to corroborate the experimental results, DFT calculations were used to determine spin densities at the metal centers in **1** and **2**. DFT calculations were carried out on **1** and **2** at the B3LYP level using the ORCA 2.8 package (Supporting Information).⁴⁷ Löwdin population analysis provides spin densities of 3.68 and 2.65 for the Fe and Co centers in **1** and **2**, respectively (Figure 3). DFT results thus support all experimental data and confirm that the spin density is predominantly located at the metal centers in these HS Fe(II) and HS Co(II) complexes.

Ethylene Homopolymerization. Fe(II) and Co(II) complexes containing nitrogen-rich ligands and dissociable

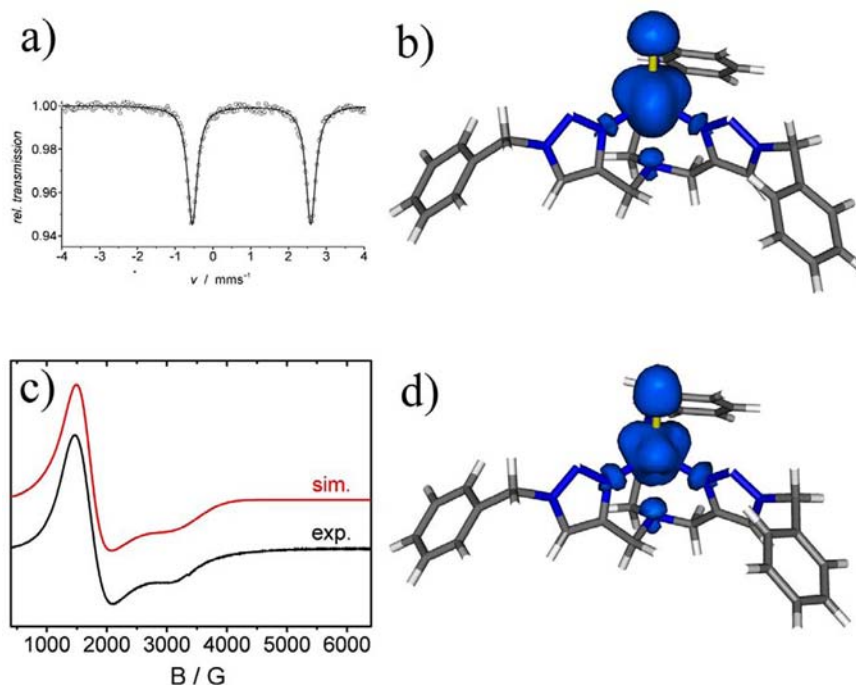


Figure 3. (a) ^{57}Fe Mössbauer spectrum of **1** recorded at 7 K. (b) DFT-calculated spin density distribution of **1**. (c) X-band EPR spectrum of **2** at 110 K recorded as a powder. (d) DFT-calculated spin density distribution of **2**.

halides are known to be effective precatalysts for homopolymerization of ethylene.⁴⁸ The presence of a tripodal platform around the metal center with a dissociable chloride ligand attached to the metal center prompted us to test the activity of both **1** and **2** as precatalysts for ethylene homopolymerization in the presence of MAO as a cocatalyst. Both **1** and **2** showed a very moderate activity of $\leq 20 \text{ kg}_{\text{polymer}}/\text{mol}_{\text{cat}}\cdot\text{h}$ as precatalysts for homopolymerization of ethylene in the presence of MAO as cocatalyst (Table 2 and Supporting Information).

Table 2. Homopolymerization of Ethylene Using Co (2) and Fe (1) Catalysts^a

| no. | catalyst | cat:MAO | T (°C) | activity ^b | T_m [°C] ^c |
|-----|---------------------------------|---------|----------|-----------------------|-------------------------|
| 1 | 2 (2.7 μmol) | 1:2000 | 50 | 20 | 132 |
| 2 | 2 (2.7 μmol) | 1:2000 | 80 | 18 | 136 |
| 3 | 1 (2.8 μmol) | 1:2000 | 50 | 10 | 130 |
| 4 | 1 (2.8 μmol) | 1:2000 | 80 | 18 | 131 |

^aPolymerizations were carried out in 250 mL of toluene for 1 h at 4 bar ethylene pressure. ^bActivity = $\text{kg}_{\text{polymer}}/\text{mol}_{\text{cat}}\cdot\text{h}$. ^cMeasured by DSC.

Analyses of the resulting polymers by ^{13}C NMR spectroscopy (Supporting Information) interestingly showed that the Fe-containing precatalyst **1** produced only linear polymers, whereas the Co-containing catalyst **2** produced slightly branched polymers (20 branches/1000 ethylenes). By increasing the polymerization temperature from 50 to 80 °C, the activity of the Co catalyst increased slightly; however, all resulting polymers were very poorly soluble in chlorinated solvents (1,1,2,2-tetrachloroethane and 1,2,4-trichlorobenzene), thereby impeding the recording of high-quality NMR spectra. Furthermore, no relevant GPC data could be recorded. ^{13}C NMR measurements again suggest a branched structure (20 branches/1000 ethylenes) for PE obtained by action of the Co catalyst (Supporting Information).^{49–51} Interestingly, the Fe

catalyst used at 80 °C produced a linear polymer. The corresponding ^{13}C NMR spectra are enclosed in the Supporting Information. In order to verify the effect of the ligand tbta on the observed catalytic activity blind catalytic runs were carried out using the corresponding metal salts without the ligand tbta. Reactions carried out using either FeCl_2 or CoCl_2 under otherwise identical conditions did not yield any significant amount of polyethylene neither at $T = 50$ nor 80 °C. Using a catalyst:MAO ratio of 1:2000, activities were $\leq 0.3 \text{ kg}_{\text{polymer}}/\text{mol}_{\text{cat}}\cdot\text{h}$ throughout. These results clearly demonstrate the requirement of the ligand tbta for achieving catalytic activity in ethylene polymerization.

1 and **2** showed no activity in the homopolymerization of styrene, cyclopentene, or *cis*-cyclooctene (Supporting Information).

CONCLUSIONS

In summary, we presented here the first examples of pseudotetrahedral HS Fe(II) and Co(II) complexes containing the tripodal tbta ligand. The complexes display a 3-fold symmetry in solution as has been observed with ^1H NMR spectroscopy. Structural parameters obtained for the Co(II) complex show that the coordination geometry around the metal center is similar to reported 5-fold-coordinated Co(II) complexes with the related amtp ligand. A combination of structural, magnetic, spectroscopic data and DFT calculations unequivocally establishes the coordination, oxidation, and spin states of these molecules. Both complexes show moderate activities as precatalysts in ethylene homopolymerization. Intriguingly, the Fe(II) complex produces only linear polymers, whereas the Co(II) complex produces slightly branched polymers. The importance of the ligand tbta has been verified by performing blind catalytic runs with ligand-free salts which show negligible catalytic activity. In view of the modular synthesis afforded by the “Click” method, it will be intriguing to

see if other substituents on the tripodal ligands would deliver better polymerization catalysts. In addition, the present complexes can also be envisaged for small molecule activation. Current work in our laboratories is directed in both directions.

EXPERIMENTAL SECTION

Materials and General Methods. The ligand *tbta* was synthesized according to a published procedure.³⁷ All solvents used during the metalation reaction were dried and distilled under argon and degassed by common techniques before use. Other chemicals and solvents were reagent grade and used as received. HPLC-grade solvents were used for spectroscopic studies. EPR spectra in the X band were recorded with a Bruker System EMX. Elemental analyses were performed with a Perkin-Elmer Analyzer 240.

Magnetic Susceptibility Measurements. Temperature-dependent magnetic susceptibility measurements were carried out with a Quantum-Design MPMS-XL-5 SQUID magnetometer equipped with a 5 T magnet in the range from 295 to 2.0 K at a magnetic field of 0.5 T. The powdered sample was contained in a gel bucket and fixed in a nonmagnetic sample holder. Each raw data file for the measured magnetic moment was corrected for the diamagnetic contribution of the sample holder and gel bucket. The molar susceptibility data were corrected for the diamagnetic contribution.

Magnetic parameters were determined using a fitting procedure to the spin Hamiltonian for zero-field splitting and Zeeman interaction $\hat{H} = D[\hat{S}_z^2 - 1/3S(S + 1)] + g\mu_B\hat{S}\cdot B$.

Temperature-independent paramagnetism (*TIP*) was included according to $\chi_{\text{calc}} = \chi + \text{TIP}$. Simulation of the experimental magnetic data with a full-matrix diagonalization of exchange coupling and Zeeman splitting was performed with the *JulX* program (E. Bill, Max-Planck Institute for Bioinorganic Chemistry, Mülheim/Ruhr, Germany).

Mössbauer Spectroscopy. Mössbauer spectra were recorded with a ⁵⁷Co source in a Rh matrix using an alternating constant acceleration *Wissel* Mössbauer spectrometer operated in the transmission mode and equipped with a *Janis* closed-cycle helium cryostat. Isomer shift is given relative to iron metal at ambient temperature. Simulation of the experimental data was performed with the *Mfit* program (E. Bill, Max-Planck Institute for Bioinorganic Chemistry, Mülheim/Ruhr, Germany).

Synthesis. [*Fe*(*TBTA*)Cl](*BF*₄), **1**. Under an argon atmosphere FeCl₂ (30 mg, 0.24 mmol), Fe(*BF*₄)₂·6H₂O (79.8 mg, 0.24 mmol), and *TBTA* (250 mg, 0.48 mmol) were dissolved in CH₃CN (10 mL). The solution was stirred at room temperature for 2 h. Then diethyl ether (15 mL) was added, and the white product was precipitated. It was filtered, washed with ether, and isolated in 80% yield (272 mg). Anal. Calcd for C₃₀H₃₀BClFeF₄N₁₀: C, 50.84; H, 4.27; N, 19.76. Found C, 50.61; H, 4.53; N, 19.37. ¹H NMR (CD₃CN, δ/ppm): 74.42 (s), 29.87 (s), 11.30 (s), 7.33 (s), 6.92 (s), 6.40 (s).

[*Co*(*TBTA*)Cl](*BF*₄), **2**. CoCl₂·6H₂O (112 mg, 0.47 mmol), Co(*BF*₄)₂·6H₂O (160 mg, 0.47 mmol), and *TBTA* (500 mg, 0.94 mmol) were dissolved in CH₃CN (30 mL). The solution was stirred at room temperature for 2 h. Then diethyl ether (50 mL) was added, and the purple product was precipitated. It was filtered, washed with ether, and isolated in 75% yield (502 mg). Single crystals suitable for X-ray diffraction were grown by slow diffusion of diethyl ether into an acetonitrile solution. Anal. Calcd for C₃₀H₃₀BClCoF₄N₁₀: C, 50.62; H, 4.25; N, 19.68. Found C, 50.35; H, 4.39; N, 19.46. ¹H NMR (CD₃CN, δ/ppm): 112.63 (s), 26.42 (s), 11.06 (s), 6.58 (s), 6.27 (s), 4.90 (s).

X-ray Crystallography. Suitable crystals for X-ray analysis of all compounds were obtained as described above. Intensity data were collected at 100(2) K on a Kappa CCD diffractometer (graphite monochromated Mo K α radiation, $\lambda = 0.71073$ Å) for **2** and at 133(2) K on a Stoe IPDS II (graphite-monochromated Mo K α radiation, $\lambda = 0.71073$ Å) for *tbta*. Crystallographic and experimental details for the structures are summarized in Table S1, Supporting Information. Structures were solved by direct methods (SHELXS-97) and refined by full-matrix least-squares procedures (based on *F*², SHELXL-97).⁵² CCDC 804879 and 804876 contain the cif files for this manuscript. All

data can be obtained free of charge from the Cambridge Crystallographic Data Centre via www.ccdc.cam.ac.uk/data_requests/cif.

ASSOCIATED CONTENT

Supporting Information

Crystallographic, DFT details, and polymerization experiments. This material is available free of charge via the Internet at <http://pubs.acs.org>.

AUTHOR INFORMATION

Corresponding Author

*Email: biprajit.sarkar@fu-berlin.de.

Notes

The authors declare no competing financial interest.

ACKNOWLEDGMENTS

We are indebted to the Fonds der Chemischen Industrie (FCI) for financial support of this project (Chemiefondsstipendium for D. S. and Liebig-Fellowship for M.M.K.). Dr. I. Hartenbach and Dr. S. Strobel are kindly acknowledged for crystal structure determination of **2**. We are grateful to the bw GRID for access to computer clusters. Special thanks to Dr. D. Wang for running some of the homopolymerization and NMR experiments.

REFERENCES

- (1) Rostovtsev, V.; Green, L. G.; Fokin, V. V.; Sharpless, K. B. *Angew. Chem., Int. Ed.* **2002**, *41*, 2596.
- (2) Tornøe, C. V.; Christensen, C.; Meldal, M. *J. Org. Chem.* **2002**, *67*, 3057.
- (3) Liang, L.; Astruc, D. *Coord. Chem. Rev.* **2011**, *255*, 2933.
- (4) Struthers, H.; Mindt, T. L.; Schibli, R. *Dalton Trans.* **2010**, *39*, 675.
- (5) Fletcher, J. T.; Bumgarner, B. J.; Engels, N. D.; Skoglund, D. A. *Organometallics* **2008**, *27*, 5430.
- (6) Schulze, B.; Friebe, C.; Hager, M. D.; Winter, A.; Hoogenboom, R.; Goerls, H.; Schubert, U. S. *Dalton Trans.* **2009**, 787.
- (7) Li, Y.; Huffman, J. C.; Flood, A. H. *Chem. Commun.* **2007**, 2692.
- (8) Meudtner, R. M.; Ostermeier, M.; Goddard, R.; Limberg, C.; Hecht, S. *Chem.—Eur. J.* **2007**, *13*, 9834.
- (9) Happ, B.; Friebe, C.; Winter, A.; Hager, M. D.; Hoogenboom, R.; Schubert, U. S. *Chem. Asian J.* **2009**, *4*, 154.
- (10) Ostermeier, M.; Berlin, M.-A.; Meudtner, R. M.; Demeshko, S.; Meyer, F.; Limberg, C.; Hecht, S. *Chem.—Eur. J.* **2010**, *16*, 10202.
- (11) Kiplin, K. J.; Crowley, J. D. *Polyhedron* **2010**, *29*, 3111.
- (12) Kiplin, K. J.; Gavey, E. L.; McAdam, C. J.; Anderson, C. B.; Lind, S. J.; Keep, C. C.; Gordon, K. C.; Crowley, J. D. *Inorg. Chem.* **2011**, *50*, 6334.
- (13) Urankar, D.; Pinter, P.; Pevec, A.; Proft, F. D.; Turel, L.; Kosmrlj, J. *Inorg. Chem.* **2010**, *49*, 4820.
- (14) Urankar, D.; Pevec, A.; Kosmrlj, J. *Eur. J. Inorg. Chem.* **2011**, 1921.
- (15) Schweinfurth, D.; Pattacini, R.; Strobel, S.; Sarkar, B. *Dalton Trans.* **2009**, 9291.
- (16) Schweinfurth, D.; Strobel, S.; Sarkar, B. *Inorg. Chim. Acta* **2011**, *374*, 253.
- (17) Obata, M.; Kitamura, A.; Mori, A.; Kameyama, C.; Czaplowska, J. A.; Tanaka, R.; Kinoshita, I.; Kusumoto, T.; Hashimoto, H.; Harada, M.; Mikita, Y.; Funabiki, T.; Yano, S. *Dalton Trans.* **2008**, 3292.
- (18) Chan, T. R.; Hilgraf, R.; Sharpless, K. B.; Fokin, V. V. *Org. Lett.* **2004**, *6*, 2853.
- (19) Demko, Z. P.; Sharpless, K. B. *Angew. Chem., Int. Ed.* **2002**, *41*, 2110.
- (20) Shearer, J.; Zhang, C. X.; Zakharov, L. N.; Rheingold, A. L.; Karlin, K. D. *J. Am. Chem. Soc.* **2005**, *127*, 5469.

- (21) Hirai, Y.; Kojima, T.; Mizutani, Y.; Shiota, Y.; Yoshiwaza, K.; Fukuzumi, S. *Angew. Chem., Int. Ed.* **2008**, *47*, 5772.
- (22) Kojima, T.; Morimoto, T.; Sakamoto, T.; Miyazaki, S.; Fukuzumi, S. *Chem.—Eur. J.* **2008**, *14*, 8904.
- (23) Kojima, T.; Amano, T.; Ishii, Y.; Ohba, M.; Okaue, Y.; Matsuda, Y. *Inorg. Chem.* **1998**, *37*, 4076.
- (24) Weisser, F.; Huebner, R.; Schweinfurth, D.; Sarkar, B. *Chem.—Eur. J.* **2011**, *17*, 5727.
- (25) Gorrell, I. B.; Parkin, G. *Inorg. Chem.* **1990**, *29*, 2452.
- (26) Kunishita, A.; Gianetti, T. L.; Arnold, J. *Organometallics* **2012**, *31*, 372.
- (27) Lehnert, N.; Fujisawa, K.; Solomon, E. I. *Inorg. Chem.* **2003**, *42*, 469.
- (28) Reinaud, O. M.; Theopold, K. H. *J. Am. Chem. Soc.* **1994**, *116*, 6979.
- (29) Blackman, A. G. *Polyhedron* **2005**, *24*, 1.
- (30) Mani, F.; Scapacci, G. *Inorg. Chim. Acta* **1980**, *38*, 151.
- (31) Benelli, C.; Bertini, I.; Di Vaira, M.; Mani, F. *Inorg. Chem.* **1984**, *23*, 1422.
- (32) Van Driel, G. J.; Driessen, W. L.; Reedjik, J. *Inorg. Chem.* **1985**, *24*, 2919.
- (33) Driessen, W. L.; Wiesmeijer, W. G. R.; Schipper-Zablotskaja, M.; de Graaff, R. A. G.; Reedjik, J. *Inorg. Chim. Acta* **1989**, *162*, 233.
- (34) Schweinfurth, D.; Weisser, F.; Bubrin, D.; Bogani, L.; Sarkar, B. *Inorg. Chem.* **2011**, *50*, 6114.
- (35) Geng, J.; Lindqvist, J.; Mantovani, G.; Chen, G.; Sayers, C. T.; Clarkson, G. J.; Haddleton, D. M. *QSAR Comb. Sci.* **2007**, *26*, 1220.
- (36) Donnelly, P. S.; Zannata, S. D.; Zammit, S. C.; White, J. M.; Williams, S. J. *Chem. Commun.* **2008**, 2459.
- (37) (a) Chan, T. R.; Hilgraf, R.; Sharpless, K. B.; Fokin, V. V. *Org. Lett.* **2004**, *6*, 2853. (b) Demko, Z. P.; Sharpless, K. B. *Angew. Chem., Int. Ed.* **2002**, *41*, 2110.
- (38) Kooistra, T. M.; Hekking, K. F. W.; Knijnenburg, Q.; de Bruin, B.; Budzelaar, P. H. M.; de Gelder, R.; Smits, J. M. M.; Gal, A. W. *Eur. J. Inorg. Chem.* **2003**, 648.
- (39) Davies, C. J.; Solan, G. A.; Fawcett, J. *Polyhedron* **2004**, *23*, 3105.
- (40) Massoud, S. S.; Broussard, K. T.; Mautner, F. A.; Vicente, R.; Saha, M. K.; Bernal, I. *Inorg. Chim. Acta* **2008**, *361*, 123.
- (41) Yang, G. J. *Chem. Crystallogr.* **2004**, *34*, 269.
- (42) Ruman, T.; Ciunik, Z.; Wolowicz, S. *Eur. J. Inorg. Chem.* **2003**, 2475.
- (43) Krzystek, J.; Swenson, D. C.; Zvyagin, S. A.; Smirnov, D.; Ozarowski, A.; Telser, J. *J. Am. Chem. Soc.* **2010**, *132*, 5241.
- (44) Jevric, M.; Zheng, T.; Meher, N. K.; Fettingner, J. C.; Mascal, M. *Angew. Chem., Int. Ed.* **2011**, *50*, 717.
- (45) Hua, Y.; Flood, A. H. *Chem. Soc. Rev.* **2010**, *39*, 1262.
- (46) Ward, A. L.; Elbaz, L.; Kerr, J. B.; Arnold, J. *Inorg. Chem.* **2012**, *51*, 4694.
- (47) Neese, F. *ORCA—an Ab Initio, Density Functional and Semiempirical Program Package*, version 2.8; Institut für Physikalische und Theoretische Chemie, Universität Bonn: Germany, Feb 2011.
- (48) Britovsek, G. J. P.; Bruce, M.; Gibson, V. C.; Kimberley, B. S.; Maddox, P. J.; Mastroianni, S.; McTavish, S. J.; Redshaw, C.; Solan, G. A.; Strömberg, S.; White, A. J. P.; Williams, D. J. *J. Am. Chem. Soc.* **1999**, *121*, 8728.
- (49) Izzo, L.; Caporaso, L.; Senatore, G.; Oliva, L. *Macromolecules* **1999**, *32*, 6913.
- (50) Möhring, V. M.; Fink, G. *Angew. Chem., Int. Ed.* **1985**, *24*, 1001.
- (51) Nodono, M.; Novak, B. M.; Boyle, P. T. *Polym. J.* **2004**, *36*, 140.
- (52) Sheldrick, G. M. *Acta Crystallogr.* **2008**, *A64*, 112.